

2013-09-01

Cadmium contamination of agricultural soils and crops resulting from sphalerite weathering.

Robson, TC

<http://hdl.handle.net/10026.1/4355>

10.1016/j.envpol.2013.09.001

Environ Pollut

All content in PEARL is protected by copyright law. Author manuscripts are made available in accordance with publisher policies. Please cite only the published version using the details provided on the item record or document. In the absence of an open licence (e.g. Creative Commons), permissions for further reuse of content should be sought from the publisher or author.

1 Disclaimer: This is a pre-publication version. Readers are recommended to consult
2 the full published version for accuracy and citation. Published in Environmental
3 Pollution, 184, 283-289 (2014), doi: 10.1016/j.envpol.2013.09.001.
4

5 **Cadmium contamination of agricultural soils and crops** 6 **resulting from sphalerite weathering**

7 T.C. Robson^{a*}, C.B. Braungardt^a, J. Rieuwerts^a, P. Worsfold^a

8

9 ^a Biogeochemistry Research Centre, Plymouth University, Drake Circus. Plymouth, PL4
10 8AA, United Kingdom.

11

12 *thomas.robson@plymouth.ac.uk

13 charlotte.braungardt@plymouth.ac.uk

14 john.rieuwerts@plymouth.ac.uk

15 P.Worsfold@plymouth.ac.uk

16

17 *Corresponding author: Thomas C. Robson Tel: (+44)7712 599565; School of
18 Geography, Earth and Environmental Science, Plymouth University, Drake Circus,
19 Plymouth, Devon, PL4 8AA.

20

21

22

23 **Abstract**

24 The biogeochemistry and bioavailability of cadmium, released during sphalerite
25 weathering in soils, were investigated under contrasting agricultural scenarios to assess
26 health risks associated with sphalerite dust transport to productive soils from mining.

27 Laboratory experiments (365 d) on temperate and sub-tropical soils amended with
28 sphalerite ($< 63 \mu\text{m}$, 0.92 wt.% Cd) showed continuous, slow dissolution ($0.6 - 1.2 \% \text{ y}^{-1}$). Wheat grown in spiked temperate soil accumulated $\approx 38 \%$ ($29 \mu\text{mol kg}^{-1}$) of the
29 liberated Cd, exceeding food safety limits. In contrast, rice grown in flooded sub-tropical
30 soil accumulated far less Cd ($0.60 \mu\text{mol kg}^{-1}$) due to neutral soil pH and Cd bioavailability
31 was possibly also controlled by secondary sulfide formation. The results demonstrate
32 long-term release of Cd to soil porewaters during sphalerite weathering. Under oxic
33 conditions, Cd may be sufficiently bioavailable to contaminate crops destined for human
34 consumption; however flooded rice production limits the impact of sphalerite
35 contamination.
36

37

38 Capsule:

39

40 Sphalerite dissolves steadily in oxic agricultural soils and can release highly bioavailable
41 Cd, which may contaminate food crops destined for human consumption.

42

43 Keywords: metals; sulfide weathering; human health; rice; risk assessment

44

45

46 **Introduction**

47 Cadmium (Cd) is considerably environmentally mobile, bioavailable and toxic to humans
48 (Smolders and Mertens, 2013) and there are linkages between mineral exploitation, Cd
49 soil contamination and human health hazards, for example the contamination of soils by
50 Japan's Jinzu River and its association with the debilitating 'itai-itai' disease (Ishihara et
51 al., 2001). In the region bordering Guangdong and Hunan provinces (China), decades of
52 metal production were shown to have contaminated river sediments and agricultural
53 soils (e.g. Chenzhou) as far as 60 km from the source ($> 9 \mu\text{mol Cd kg}^{-1}$) (Limei et al.,
54 2008) and inhabitants are considered at risk of chronic health effects from consuming
55 locally grown rice and vegetables (H. Zhao et al., 2012; Zhuang et al., 2009). Crop safety
56 is a concern because the primary human intake routes for Cd are tobacco smoking and
57 diet (Järup, 2003), both of which link human exposure to soil contamination. Chronic

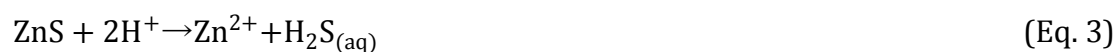
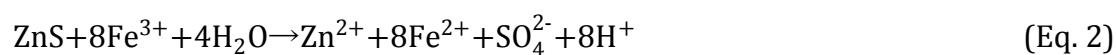
58 toxicity may arise because Cd has a long biological half-life (15 – 30 years) and
59 accumulates in the body, resulting in kidney disease, osteoporosis, lung and prostate
60 cancer and endocrine disruption (Henson and Chedrese, 2004; Järup, 2003).

61
62 Mining and ore processing produces fine mineral particles enriched with potentially
63 toxic metals and metalloids (e.g. As, Cd, Hg). These particles are vulnerable to fluvial
64 (Miller et al., 2004; Simmons et al., 2005) and aeolian (Castillo et al., 2013; Zota et al.,
65 2009) transport, for example through erosion from exposed tailings, so they can behave
66 as vectors for toxic elements. Several investigators have reported the spatial distribution
67 and concentration of toxic metals in soils affected by mineral exploitation, but less is
68 understood about how transported mineral particles influence soil quality in terms of
69 the biogeochemical cycling of toxic metals and the risk they pose to human health
70 through crop contamination.

71
72 Commonly exploited sulfide ores (e.g. sphalerite) are vulnerable to oxidative and acid-
73 promoted dissolution under moist, oxic surface conditions and may release metals into
74 soil porewater and surface waters, providing a source of potentially toxic metals for
75 plant uptake. This situation is most likely to affect communities in developing and
76 rapidly industrialising countries, where environmental regulations may be either weak
77 or poorly enforced and soils impacted by mining may be used for agriculture (Miller et
78 al., 2004; Zhuang et al., 2009).

79
80 Sphalerite (ZnS), the primary geologic source of zinc (Zn) and Cd, occurs commonly
81 around the world. Sphalerite is notable for its tendency for isomorphic substitution of
82 Zn by other metals and Cd is generally present in solid solution at 0.2–1 % (Smolders
83 and Mertens, 2013). The alteration mechanisms proposed for sphalerite include
84 oxidative dissolution, either by molecular oxygen (Eq. 1) or Fe(III) (Eq. 2), and acid-
85 promoted dissolution (Eq. 3) (Heidel et al., 2011). Cd is released from solid solution
86 during sphalerite dissolution (Stanton et al., 2008).

87



88
89 Laboratory experiments in aqueous media (Acero et al., 2007; Stanton et al., 2008)
90 showed that sphalerite dissolution follows a first order reaction with respect to $[\text{H}^+]$ (pH
91 1 – 4.2); the rate increases with temperature (25 – 70 °C) and is independent of
92 dissolved oxygen concentrations (6.3 – 270 μM dO_2), suggesting that the process
93 described by Eq. 1 is of minimal importance. Apart from differences in experimental
94 design, the iron (Fe) content of the sphalerite is also proposed to influence the
95 dissolution rate (Weisener et al., 2003).

96
97 The aim of this study was to determine the rate of sphalerite dissolution and Cd release
98 in soils of contrasting geologic and climatic provenance, and the bioavailability of the Cd
99 to key crops under relevant agricultural scenarios.

100 **Methods**

101 **Investigative approach**

102 This study comprised of: (1) Laboratory batch incubations of sphalerite-spiked (0.1 %
103 m/m) soils to determine sphalerite dissolution behaviour and (2) Phytoavailability
104 experiments where *Triticum aestivum* (spring wheat) and *Oryza sativa* (rice) were
105 grown in samples of the temperate and flooded sub-tropical soils, respectively, to
106 evaluate the bioavailability of Cd released from sphalerite.

107 **Reagents and materials**

108 Reagents were of analytical grade or higher (ROMIL, Sigma-Aldrich, Fisher) and ultra-
109 high purity water (UHP, $\geq 18.2 \text{ M}\Omega \text{ cm}^{-1}$) was used for all experiments. Specimen
110 sphalerite was obtained from a private collection (Richard Tayler Minerals, Cobham,
111 UK).

112 **Soil and mineral sampling, preparation and characterisation**

113 A temperate soil (inceptisol from the Tamar Valley, Cornwall, United Kingdom) was
114 sampled from low-intensity grassland, used only for haymaking for the past decade. The
115 sub-tropical soil (The University of Hong Kong Kadoorie Centre) comprised sub-surface
116 oxisol from secondary forest and horticultural soil, in equal parts by volume.

117

118 Experimental soils (< 2 mm, dried at 40 °C) were fertilised with dried (50 °C, ≥ 72 h)
119 well-rotted animal dung (milled and sieved to < 2 mm) at 10 % m/m, bringing the
120 organic matter content to the upper range for productive soils. Sphalerite was finely
121 ground, sieved (ball mill, < 63 µm) and stored in a desiccating, N₂-purged atmosphere
122 (see Laboratory batch incubation experiments). The < 63 µm fraction represents clay
123 and silt size particles, which are thought to account for the majority of fugitive dust mass
124 flux (Kon et al., 2007).

125

126 Experimental soils were characterised using standard methods (Carter and Gregorich,
127 2007): total sulfur (S), nitrogen, organic/inorganic carbon (NC2500 elemental analyser,
128 Carlo Erba), eCEC, organic matter, texture and pH (United States Environmental
129 Protection Agency, 2004). For elemental analyses, soils and sphalerite were microwave-
130 digested (MarsXpress, CEM) in 50 % v/v 1:3 HNO₃:HCl. Bulk mineralogy was evaluated
131 using powder X-ray diffraction (XRD) (Cu-Kα, 2-70° 2θ, 0.02°/S, D5000, Siemens). The
132 sphalerite was also examined using scanning electron microscopy with energy
133 dispersive spectroscopy (SEM-EDS) (JSM-7100F, JEOL/Aztec EDS, Oxford Instruments).

134 **Laboratory batch incubation experiments**

135 Batch incubations (≤ 12 months) were conducted in polypropylene beakers using 100 g
136 aliquots of the experimental soils. The soils were either spiked with 0.1 g ground
137 sphalerite or left as controls (no ZnS) and then their moisture was maintained
138 gravimetrically at 75 % field capacity. Triplicate incubation batches were sacrificed and
139 analysed after 0 hours, 7, 30, 90, 180, 270 and 365 days under laboratory conditions.
140 Sacrificed soils were freeze-dried, homogenized and sub-sampled for analyses. Soluble
141 major ions (NO₃⁻, SO₄²⁻), cation-exchangeable Cd/Zn and EDTA-extractable Cd/Zn were
142 extracted in UHP water (1:5), 0.01 M CaCl₂ (1:5) and 0.1 M EDTA (1:30, pH 7.5),

143 respectively (2 h agitation, reciprocating shaker). Extracts were centrifuged, filtered
144 (0.45 μm) and preserved until analysis (freezing, acidification or refrigeration).

145

146 An abiotic control experiment, analogous to the first 30 days of the batch incubation
147 experiments, was performed using sterile soils. Soils were fractionally sterilised to
148 ensure overkill of both microorganisms and endospores, using three cycles of steam
149 heating (97 ± 2 °C, 2 h) and overnight incubated (37 ± 1 °C). The incubations were
150 performed in autoclaved (121 °C, 1 h), foam-bunged (tortuous path filter) glass conical
151 flasks. Sterility was maintained by using only heat-sterilised (≥ 250 °C) implements,
152 filter-sterilised (0.22 μm) water and observing best practise for sterile handling.

153 **Phytoavailability experiments**

154 Larger (2 kg), analogous, soil incubations were established in polypropylene pots and
155 maintained in parallel with those of the batch experiment. After 180 days, 10-day wheat
156 seedlings (350 seeds m^{-2}) were transplanted into the temperate soils. The plants were
157 matured to ripeness (112 days) under glasshouse conditions (24 ± 3 °C, 66 ± 3 % RH)
158 and then the stems and ears were rinsed (≥ 5 times) with water and freeze-dried. The
159 tissues were comminuted (food processor) and 0.5 ± 0.01 g ($n = 3$) of tissue was
160 microwave-digested in 10 mL HNO_3 (50 % v/v conc.).

161

162 The sub-tropical soils received 14-day rice seedlings, were flooded with 6 cm standing
163 water and plants matured (152 days) inside a growth chamber (Fitotron PG660, Sanyo;
164 16 h light, 8 h dark at 27 °C, followed by 12 h light, 12 h dark at 24 °C) and then treated
165 as per the wheat. The drained, saturated soils were core-sampled (\varnothing 2.5 cm, $n = 5$)
166 inside an anoxic chamber (Coy laboratory products). Bulked cores were sub-sampled for
167 aqueous extraction, capped and sealed with Parafilm and then extracted as previously
168 described (see Laboratory batch incubation experiments). Dissolved sulfide was
169 determined in soil water extracts (in an anoxic chamber) using the methylene blue
170 method (Cline, 1969). Solid-phase Fe speciation and acid-volatile sulfide were
171 determined after Lovley and Phillips (1986) and Allen et al. (1993), respectively.
172 Porewater pH and Eh were determined in the water that collected in the core voids.

173 **Analytical techniques**

174 Anion, Fe (II) and dissolved sulfide (S^{2-}) concentrations were determined using ion
175 chromatography (DX-500, Dionex Corporation) or spectrophotometry (8453 UV-Vis,
176 Agilent), respectively. Aqueous metal concentrations were determined using ICP-OES
177 (725-ES, Varian) and ICP-MS (X-series 2 + Collision Cell, Thermo Scientific). Half-cell
178 redox potentials (Hanna HI9025, BDR Gelplas ORP) were corrected against ZoBell's
179 solution. Certified reference materials (BCR 320R channel sediment, IRMM 804 rice
180 flour and PACS-1 marine sediment) were used to verify the satisfactory accuracy and
181 performance of the methods (Table S1). Statistical analyses were performed using the
182 Sigmaplot 12 software package (Systat Software).

183 **Results and discussion**

184 **Experimental soil and sphalerite characterisation**

185 Both experimental soils were of circum-neutral pH, rich in organic matter, with a similar
186 moderate eCEC (Table 1). Both soils were Fe rich (5.5 – 6.3 % Fe m/m) but the sub-
187 tropical soil contained 7 times less manganese, more aluminium (6.2 % vs. 3.9 %) and a
188 lower proportion of poorly crystalline Fe and aluminium oxides/hydroxides (factor of 2
189 – 4). Both soils had similar S, Zn and Cd concentrations, which fell within (Cd) or just
190 above (Zn) the range expected for uncontaminated soils (Mertens and Smolders, 2013).
191 The main crystalline phases were clinocllore ($(Mg,Fe^{2+})_5Si_3Al_2O_{10}(OH)_8$), muscovite
192 ($KAl_2(AlSi_3O_{10})(OH)_2$), illite ($(K,H_3O)(Al,Mg,Fe)_2(Si,Al)_4O_{10}[(OH)_2,(H_2O)]$) and quartz
193 (SiO_2) in the temperate soil (sandy loam) and kaolinite ($Al_2Si_2O_5(OH)_4$), orthoclase
194 ($KAlSi_3O_8$), microcline ($KAlSi_3O_8$), gibbsite ($Al(OH)_3$) and quartz in the sub-tropical soil
195 (silt loam).

196

197 Elemental (wet) analyses and SEM-EDS examination showed that the experimental
198 mineral consisted of ZnS ($Zn_{1.01}S_{0.99}$) with 0.3 % m/m Fe and 0.9 % m/m Cd. An XRD
199 analysis and reference to mineral databases also confirmed the crystalline structure to
200 be that of sphalerite and not the sphalerite polymorph, wurtzite (Figure S1).

201 **Soil biogeochemical conditions throughout oxic incubations**

202 The pH was not controlled during the experiment and a notable decrease was observed
203 in the pH of both temperate (- 1.05 pH units) and sub-tropical (- 0.43 pH units) soils
204 during the initial 30 days of incubation. After 30 days, the temperate and sub-tropical
205 soils fluctuated around pH 5.53 ± 0.13 and pH 6.40 ± 0.08 , respectively. Acid buffering
206 experiments, performed after Magdoff and Bartlett (1985), demonstrated that the sub-
207 tropical soil had significantly greater buffering capacity ($\approx 43\%$ at neutral-acid pH) than
208 the temperate soil, which was devoid of carbonate, partly explaining the disparate pH
209 decline in the early stages of the experiment (Figure S2).

210

211 Data from an abiotic control experiment covering the initial 30 days incubation of the
212 temperate soil (Figure 1) indicate that the pH decline was mediated by soil microbiota,
213 and was coupled with sharp increases in nitrate and sulfate concentrations, reflecting
214 ammonium and sulfur-oxidising bacterial activity. Both can contribute to soil acidity
215 especially if percolation is prevented, as was the case in these experiments.

216 [Approximate location for Figure 1]

217 Sphalerite dissolution had a negligible effect on soil pH, since control and spiked
218 incubation soil pH generally differed by < 0.1 pH unit throughout the batch incubations.
219 Redox potential (Eh) was determined in soil extracts, which were performed as for the
220 pH determinations (see Soil and mineral sampling, preparation and characterisation).
221 The data indicated consistently oxic conditions (350 – 400 mV) throughout the
222 experiment.

223 **Geochemical conditions in sub-tropical soil during rice cultivation**

224 After rice cultivation (180 days oxic, 152 days flooded) the sub-tropical soils had
225 attained neutral pH (7.01 ± 0.08) and moderately reducing conditions (Eh - 23 ± 6 mV)
226 (Figure 2 b). Flooded paddy soils often attain neutral pH as many important reduction
227 reactions, e.g. $\text{Fe(III)} > \text{Fe(II)}$, consume free protons (Ponnamperuma, 1972).

228 [Approximate location for Figure 2.]

229 Redox indicators and CaCl₂-extractable metal concentrations suggest that the
230 availability of Cd in porewater, and therefore to the rice plants, was limited by the
231 formation of secondary Fe/Cd/Zn sulfide phases. Depleted soluble nitrate (> 99 %) and
232 sulfate (≥ 94 %) (Figure 2 a), together with a significant proportion of acid-extractable
233 Fe(II) (66 ± 10 %), indicated the influence of nitrate, Fe and sulfate-reducing anaerobes
234 (Inglett et al., 2005). No dissolved sulfide was detected in soil extracts but acid-volatile
235 sulfide (AVS) was found in the reduced control soils (200 ± 16 μmol S²⁻ kg⁻¹), providing
236 evidence for the formation of amorphous secondary sulfides (e.g. greigite, mackinawite).
237 An AVS determination was not possible in the spiked soils because sphalerite itself is
238 acid-volatile. Concurrent with sulfide formation, net (control-corrected) CaCl₂-
239 extractable Cd and Zn concentrations were considerably lower in the reduced soils,
240 compared with their oxic equivalents (Figure 2 c), and net EDTA-extractable Cd (Cd_{net})
241 concentrations also fell from 0.23 ± 0.02 to 0.12 ± 0.02 μmol kg⁻¹. Much of the depleted
242 sulfate was unaccounted for by AVS formation, suggesting other contributory
243 mechanisms. There was no olfactory evidence for H₂S_(g) evolution and sulfate adsorption
244 is minimal in pH neutral soils (Scherer, 2009), excluding adsorption effects. Other
245 potential mechanisms for the observed sulfate and extractable Cd depletion were the
246 formation of non-acid-volatile sulfides (e.g. pyrite, greenockite) and plant uptake,
247 respectively, and these are given further consideration in the section 'Uptake by paddy
248 rice grown in sub-tropical soil'.

249 **Sphalerite dissolution**

250 Cd and Zn extraction protocols

251 The 0.01 M CaCl₂ protocol was applied to provide a 'snapshot' reflecting plant-available
252 concentrations at a given time (Meers et al., 2007). The 0.1 M EDTA extraction protocol
253 was selected because it effectively scavenges metal cations from solid soil phases (Lo
254 and Yang, 1999; Schecher, 2001), providing an indication of the total Cd and Zn release
255 from sphalerite and total plant-available concentrations over a longer timescale.

256 Cd and Zn release trends

257 The clear distinction between Cd concentrations obtained from control and spiked
258 incubations (Figure 3a/a_i & b/b_i) evidences the release of Cd from sphalerite
259 dissolution. This divergence can be seen after 7 days incubation of both the temperate
260 and sub-tropical soils. Cd concentrations extracted from control incubations were
261 relatively constant throughout the incubation duration, which demonstrates that Cd
262 extractability was not affected by changes in soil pH during the oxic incubations.

263

264 [Approximate location for Figure 3.]

265

266 Extractable Zn concentrations (Figure 3c/c_i & d/d_i) were considerably higher than Cd
267 concentrations, reflecting the molar Zn:Cd ratio in the sphalerite. In the temperate soil
268 (Figure 3c & d), comparison with the control shows that Zn was released from sphalerite
269 with increasing incubation time and, as with the Cd, the release curve did not exhibit a
270 change in slope over the last 180 days of the experiment. In the temperate control soils,
271 Zn concentrations from the beginning and the end of the experiment did not
272 significantly differ ($p = 0.05$).

273

274 The CaCl₂-extractable Zn concentrations in spiked sub-tropical soils were higher than in
275 the control soil (Figure 3c_i), most notably during the last 180 days of the experiment;
276 however the CaCl₂-extractable concentrations in control soils varied significantly ($p >$
277 0.05 , ANOVA) during incubation. The EDTA-extractable Zn concentrations in spiked and
278 control sub-tropical soils (Figure 3d_i) fluctuated throughout the incubation time and
279 there was no significant difference between concentrations at the beginning and end of
280 the experiment ($p < 0.05$, ANOVA). Comparison of the Zn release trends with those of Cd,
281 which were linear with incubation time, suggest that Zn released from the sphalerite
282 was in equilibrium with another solid phase and recalcitrant to EDTA complexation. The
283 net release indicated by CaCl₂-extractable concentrations (Figure 3c_i) was masked in the
284 EDTA-extractable data, as the EDTA extraction was not sensitive to minor variations in
285 Zn lability.

286 Dissolution rate, trends and limits

287 EDTA-extractable Cd concentrations were the most suitable indicator of the extent and
288 rate of sphalerite dissolution, in this case meaning alteration from the original sulfide
289 species. Unlike Zn, Cd release trends were clear and consistent (concentration vs. time)
290 in both experimental soils. Additionally, Cd release is directly correlated with sphalerite
291 dissolution rate (Stanton et al., 2008) and EDTA dissolves sphalerite oxidation products
292 but not the sulfide itself (Rumball and Richmond, 1996), as confirmed by preliminary
293 experiments (data not shown).

294
295 Net Cd release (Cd_{net}) from the sphalerite was calculated by subtracting EDTA-
296 extractable concentrations obtained from control incubations from those obtained from
297 the respective spiked incubations. The Cd_{net} data were used to estimate the percentage
298 sphalerite dissolved at each incubation time point (Table 2). The relationship between
299 Cd_{net} and incubation duration was linear ($R^2 \geq 0.96$) for both temperate and sub-tropical
300 soils, indicating a constant rate of Cd release, and therefore sphalerite dissolution,
301 throughout the experiments. Several studies on sphalerite dissolution in aqueous
302 solution showed that dissolution rates decline during the initial few hundred hours of
303 exposure and then attain an apparent steady state (Acero et al., 2007; Stanton et al.,
304 2008; Weisener et al., 2003). It was proposed that this change is concurrent with the
305 formation of Zn-deficient, polysulfide and elemental S product layers on sphalerite
306 particles, and a shift from reaction rate-limited dissolution to dissolution limited by
307 reagent diffusion (i.e. H_3O^+ , O_2 , Zn^{2+} , Cd^{2+} and/or S) through those product layers
308 (Weisener et al., 2003). Acero et al. (2007) argued that, because steady state was
309 attained, the layers were not passivating and initially high dissolution rates probably
310 resulted from micro-crystals and oxidised phases on the pre-exposure sphalerite
311 surfaces. In this study the slower dissolution rate remained constant over long durations
312 (hundreds of days), regardless of whether these product layers are porous, and
313 therefore not diffusion limiting, or whether they are in equilibrium with bulk solution,
314 and therefore do not accumulate.

315
316 The data from this study are consistent with slow steady-state dissolution. The constant
317 Cd release excludes the significant formation of stable secondary Cd phases, which

318 would have produced declining CaCl_2 and EDTA-extractable concentrations with
319 increasing incubation duration by sequestering Cd^{2+} from the porewater. The absence of
320 secondary phases was evidenced by SEM-EDS examination of sphalerite platelets
321 exposed to field conditions for 2 years. Full details of this method are provided in
322 Robson et al. (2013).

323

324 Dissolution rates observed at 365 days are indicative of the annual average,
325 approximately 1 and 0.5 $\mu\text{mol Cd g}^{-1} \text{ZnS a}^{-1}$ for the temperate and sub-tropical soils,
326 respectively. Accounting for the reducing surface area of the given mass of dissolving
327 sphalerite and assuming proportionality between dissolution rate and surface area
328 (shrinking particle model) (Pradhan et al., 2010; Safari et al., 2009), the half-life of the
329 sphalerite was estimated to be 50 and 94 years in the temperate and sub-tropical soils,
330 respectively.

331

332 The slower dissolution rates observed in the sub-tropical soil were attributed to the
333 prevailing soil pH. Based on kinetics data from Acero et al. (2007), a change in
334 porewater pH from 5.53 (temperate soil) to 6.40 (sub-tropical soil) would result in
335 dissolution rates being reduced by 66 %; therefore pH is likely to be the most significant
336 factor affecting sphalerite dissolution in oxic soils. The shift to neutral pH observed in
337 flooded sub-tropical soils (from pH 6.40) is associated with a further 53 % reduction in
338 the dissolution rate, based on pH alone.

339 **Cd uptake by crops**

340 Uptake by wheat grown in temperate soil

341 Grain and stem Cd concentrations in the spring wheat grown in the sphalerite-spiked
342 temperate soil were considerably higher (by a factor of ≥ 75) than in plants grown in the
343 control soil (Figure 4). The wheat grain contained $29.0 \pm 3.3 \mu\text{mol Cd kg}^{-1}$, around 8
344 times higher than the international food safety limit of $3.6 \mu\text{mol kg}^{-1}$ (FAO/WHO, 2006).

345

346 [Approximate location for Figure 4.]

347

348 The data suggest that high Cd concentrations in grain produced from the spiked soil
349 were proportional to the magnitude of the bioavailable Cd pool in that soil. Stem-to-
350 grain transfer factors (TF) were the same for plants grown in spiked and control soil;
351 therefore the translocation rate was independent of the phytoaccessible Cd
352 concentration in the soil and the stem Cd concentration (Figure 4).

353

354 Stem bioconcentration factors (BCF), based on Cd_{net} values, for plants grown in spiked
355 soils were 25 times higher than for those grown in control soils. The probable
356 explanation for this observation is soil 'ageing'. Cd is generally regarded as exhibiting
357 minimal ageing effect (Smolders and Mertens, 2013) but Hamon et al. (1998)
358 demonstrated that around 1 % of soil Cd could be rendered unavailable for plant uptake
359 per year of soil residence time. Ageing may have rendered the antecedent Cd in the soils
360 far less phytoavailable than the Cd recently introduced by sphalerite dissolution.

361 Uptake by paddy rice grown in sub-tropical soil

362 Rice stem and grain Cd concentrations of plants grown in spiked soils were 3 – 4 times
363 higher than in control soil plants (Figure 4). Although the plants were contaminated by
364 the sphalerite, the edible tissue concentration ($0.597 \pm 0.019 \mu\text{mol Cd kg}^{-1}$) was well
365 below applicable Chinese ($1.78 \mu\text{mol Cd kg}^{-1}$) and international ($3.56 \mu\text{mol Cd kg}^{-1}$) food
366 safety limits (FAO/WHO, 2006; USDA Foreign Agriculture Service, 2010). For
367 comparison, Cd concentrations in the wheat (spiked soil) were higher than those for rice
368 by a factor of 49 in seeds and 24 in stems. Given that the rate of sphalerite dissolution in
369 the experimental soils only varied by a factor of 2, the tissue concentrations illustrate
370 significant differences in the Cd bioavailability and/or uptake behaviour in the rice and
371 wheat soil-plant systems.

372

373 The data suggest that, all factors being equal, the rice had a propensity for Cd uptake
374 similar to or greater than the wheat. In control soils, the wheat and rice stem
375 concentrations were similar ($0.74 - 0.85 \mu\text{mol kg}^{-1} \text{Cd}$) and the rice stem BCF was much
376 higher than for the wheat (Figure 4). Also, the rice TF increased in spiked soils (+ 53 %),
377 indicating that the plants responded to higher Cd availability by enhancing stem-to-
378 grain translocation. In light of this apparent propensity for uptake, the relatively low

379 rice tissue Cd concentrations suggest that decreased Cd availability in the paddy soil
380 porewater limited uptake. This proposition is supported by CaCl₂-extractable Cd
381 concentrations that were below the detection limit (Figure 2 c), Cd_{net} concentrations
382 that were reduced by 49 % (versus oxic incubation) and stem BCF values that were the
383 same (6.36 – 6.40) in spiked and control soils (i.e. equal bioavailability).

384
385 Soil-to-rice Cd transfer was examined to determine if this could explain the depleted
386 extractable Cd concentrations obtained from the sub-tropical soils (see Geochemical
387 conditions in sub-tropical soil during rice cultivation). The plant roots were not analysed
388 but their biomass is always much smaller than the stem biomass and therefore assuming
389 equal contribution by the root and stems provided a conservative estimate (Kibria and
390 Ahmed, 2006). Although the neutral soil pH and plant uptake might explain the
391 depletion of CaCl₂-extractable Cd, these factors cannot entirely explain the decreased
392 Cd_{net}. Firstly the EDTA extraction, from which Cd_{net} is derived, would have been
393 insensitive to the shift towards neutral soil pH. Secondly, after considering the estimated
394 total Cd uptake by rice, a 33 % decrease in Cd_{net} still remained unaccounted for.
395 Therefore it is likely that the formation of non-acid-volatile secondary sulfides (see
396 Geochemical conditions in sub-tropical soil during rice cultivation) contributed to the
397 low bioavailability and rice uptake of Cd in this study (de Livera et al., 2011).

398
399 Lowland rice is traditionally grown under near-constant standing water; however
400 increasing global population and freshwater demand have catalysed the adoption of
401 new agricultural practises such as 'system of rice intensification' (SRI), a set of
402 management principles that discourage flooded agriculture (Africare et al., 2010; L. Zhao
403 et al., 2010). A shift towards more oxic soil management will remove the protective
404 biogeochemical conditions afforded by soil flooding and enhance the bioavailability of
405 Cd in soils.

406 **Conclusions**

407 Sphalerite exhibits slow, steady dissolution behaviour in oxic agricultural soils
408 developed under contrasting geoclimatic conditions and is accompanied by the release
409 of the guest element Cd. Sphalerite contamination impacts soil quality for decades to

410 centuries, long after its introduction to soils ceases. The liberated Cd is highly
411 bioavailable under oxic conditions, as indicated by *Triticum aestivum*, and has the
412 potential to contaminate crops and pose a human health hazard. Data from *Oryza sativa*
413 indicate that flooded rice production can limit these impacts by neutralising soil pH and
414 possibly by providing sulfate-reducing conditions, under which secondary Cd sulfides
415 can form. The recently publicised advantages of ending a reliance upon flooded
416 agriculture (increased yields, reduced water consumption) suggests that growing rice
417 under more oxic conditions will increase in popularity. Adopters of these new practices
418 working Cd or sphalerite-impacted soil will sacrifice the protective biogeochemical
419 conditions afforded by flooding, increasing the risk of producing contaminated food.

420

421 **Acknowledgements**

422 This research was funded by a Plymouth University PhD studentship and the Seale
423 Hayne Educational Trust Fund. The authors would like to acknowledge OEA
424 Laboratories Ltd, Kelly Bray, UK, for assistance with S analysis, and thank The University
425 of Hong Kong Kadoorie Centre for supplying soil samples. We also thank the three
426 anonymous reviewers, whose feedback helped us improve the manuscript.

427

428 **References**

429

- 430 Acero, P., Cama, J., Ayora, C., 2007. Sphalerite dissolution kinetics in acidic environment.
431 *Appl. Geochem.* 22, 1872–1883.
- 432 Africare, Oxfam America, WWF-ICRISAT Project, 2010. More Rice for People, More
433 Water for the Planet. WWF-ICRISAT Project, Hyderabad, India.
- 434 Allen, H.E., Fu, G., Deng, B., 1993. Analysis of acid-volatile sulfide (AVS) and
435 simultaneously extracted metals (SEM) for the estimation of potential toxicity in
436 aquatic sediments. *Environ. Toxicol. Chem.* 12, 1441–1453.
- 437 Carter, M.R., Gregorich, E.G., 2007. *Soil Sampling and Methods of Analysis*, 2nd ed. CRC
438 Press, Boca Raton, USA.
- 439 Castillo, S., de la Rosa, J.D., de la Campa, A.M.S., González-Castanedo, Y., Fernández-
440 Caliani, J.C., Gonzalez, I., Romero, A., 2013. Contribution of mine wastes to
441 atmospheric metal deposition in the surrounding area of an abandoned heavily
442 polluted mining district (Rio Tinto Mines, Spain). *Sci. Total. Environ.* 449, 363–372.
- 443 Cline, J.D., 1969. Spectrophotometric determination of hydrogen sulfide in natural
444 waters. *Limnol. Oceanogr.* 14, 454–458.
- 445 de Livera, J., McLaughlin, M.J., Hettiarachchi, G.M., Kirby, J.K., Beak, D.G., 2011. Cadmium
446 solubility in paddy soils: effects of soil oxidation, metal sulfides and competitive

447 ions. *Sci. Total. Environ.* 409, 1489–1497.

448 FAO/WHO, 2006. Report of the 38th session of the Codex Committee on Food Additives
449 and Contaminants. Food and Agriculture Organization of the United Nations & World
450 Health Organization, The Hague, Netherlands.

451 FAO/WHO, 2010. Summary Report of the Seventy-Third Meeting of Joint FAO/WHO
452 Expert Committee on Food Additives. Food and Agriculture Organization of the
453 United Nations & World Health Organization, The Hague, Netherlands.

454 Hamon, R.E., McLaughlin, M.J., Naidu, R., Correll, R., 1998. Long-term changes in
455 cadmium bioavailability in soil. *Environ. Sci. Technol.* 32, 3699–3703.

456 Heidel, C., Tichomirowa, M., Breitkopf, C., 2011. Sphalerite oxidation pathways detected
457 by oxygen and sulfur isotope studies. *Appl. Geochem.* 26, 2247–2259.

458 Henson, M.C., Chedrese, P.J., 2004. Endocrine disruption by cadmium, a common
459 environmental toxicant with paradoxical effects on reproduction. *Exp. Biol. Med.*
460 (Maywood) 229, 383–392.

461 Inglett, P.W., Reddy, K.R., Corstanje, R., 2005. Anaerobic soils, in: Hillel, D. (Ed.),
462 Encyclopedia of Soils in the Environment. Academic Press Inc, Waltham MA, USA, pp.
463 71–78.

464 Ishihara, T., Kobayashi, E., Okubo, Y., Suwazono, Y., Kido, T., Nishijyo, M., Nakagawa, H.,
465 Nogawa, K., 2001. Association between cadmium concentration in rice and mortality
466 in the Jinzu River Basin, Japan. *Toxicology* 163, 23–28.

467 Järup, L., 2003. Hazards of heavy metal contamination. *Br. Med. Bull.* 68, 167–182.

468 Kibria, M.G., Ahmed, M.J., 2006. Cadmium and lead uptake by rice (*Oryza Sativa* L.)
469 grown in three different textured soils. *Soil & Environ.* 25, 70–77.

470 Kon, L.C., Durucan, S., Korre, A., 2007. The development and application of a wind
471 erosion model for the assessment of fugitive dust emissions from mine tailings
472 dumps. *Int. J. Mini. Reclamat. Environ.* 21, 198–218.

473 Limei, Z., Xiaoyong, L., Tongbin, C., Xiulan, Y., Hua, X., Bin, W., Lixia, W., 2008. Regional
474 assessment of cadmium pollution in agricultural lands and the potential health risk
475 related to intensive mining activities: a case study in Chenzhou City, China. *J.*
476 *Environ. Sci. (China)* 20, 696–703.

477 Lo, I.M., Yang, X.Y., 1999. EDTA extraction of heavy metals from different soil fractions
478 and synthetic soils. *Water Air Soil Pollut.* 109, 219–236.

479 Lovley, D.R., Phillips, E.J.P., 1986. Availability of ferric iron for microbial reduction in
480 bottom sediments of the freshwater tidal Potomac River. *Appl. Environ. Microbiol.*
481 52, 751–757.

482 Magdoff, F.R., Bartlett, R.J., 1985. Soil and pH buffering revisited. *Soil Sci. Soc. Am. J.* 49,
483 145-148.

484 Meers, E., Laing, Du, G., Unamuno, V., Ruttens, A., Vangronsveld, J., Tack, F.M.G., Verloo,
485 M.G., 2007. Comparison of cadmium extractability from soils by commonly used
486 single extraction protocols. *Geoderma* 141, 247–259.

487 Mertens, J., Smolders, E., 2013. Zinc, in: Alloway, B.J. (Ed.), *Heavy Metals in Soils: Trace*
488 *Metals and Metalloids in Soils and Their Bioavailability*. Springer, Dordrecht,
489 Netherlands, pp. 465–493.

490 Miller, J.R., Hudson-Edwards, K.A., Lechler, P.J., Preston, D., Macklin, M.G., 2004. Heavy
491 metal contamination of water, soil and produce within riverine communities of the
492 Rio Pilcomayo Basin, Bolivia. *Sci. Total Environ.* 320, 189-209.

493 Ponnampereuma, F.N., 1972. The chemistry of submerged soils. *Adv. Agron.* 24, 29–88.

494 Pradhan, D., Kim, D.J., Chaudhury, G.R., Sohn, J.S., Lee, S.W., 2010. Dissolution kinetics of
495 complex sulfides using acidophilic microorganisms. *Mater. Trans.* 51, 413–419.

496 Robson, T.C., Braungardt, C.B., Keith-Roach, M.J., Rieuwerts, J.S., Worsfold, P.J., 2013.
497 Impact of arsenopyrite contamination on agricultural soils and crops. *J. Geochem.*
498 *Explor.* 125, 102–109.

499 Rumball, J.A., Richmond, G.D., 1996. Measurement of oxidation in a base metal flotation
500 circuit by selective leaching with EDTA. *Int. J. Miner. Process.* 48, 1–20.

501 Safari, V., Arzpeyma, G., Rashchi, F., Mostoufi, N., 2009. A shrinking particle - shrinking
502 core model for leaching of a zinc ore containing silica. *Int. J. Miner. Process.* 93, 79–
503 83.

504 Schecher, W., 2001. Thermochemical Data Used in MINEQL+ version 4.5. Environmental
505 Research Software, Hallowell, UK.

506 Scherer, W.H., 2009. Sulfur in soils. *J. Plant Nutr. Soil Sci.* 172, 326–335.

507 Simmons, R.W., Pongsakul, P., Saiyasitpanich, D., Klinphoklap, S., 2005. Elevated levels of
508 cadmium and zinc in paddy soils and elevated levels of cadmium in rice grain
509 downstream of a zinc mineralized area in Thailand: implications for public health.
510 *Environ. Geochem. Health* 27, 501–511.

511 Smolders, E., Mertens, J., 2013. Cadmium, in: Alloway, B.J. (Ed.), *Heavy Metals in Soils:
512 Trace Metals and Metalloids in Soils and Their Bioavailability*. Springer, Dordrecht,
513 Netherlands, pp. 283–311.

514 Stanton, M.R., Gemery-Hill, P.A., Shanks Iii, W.C., Taylor, C.D., 2008. Rates of zinc and
515 trace metal release from dissolving sphalerite at pH 2.0–4.0. *Appl. Geochem.* 23,
516 136–147.

517 United States Environmental Protection Agency, 2004. Test methods for evaluating solid
518 waste, physical/chemical methods [online]. URL
519 <http://www.epa.gov/epawaste/hazard/testmethods/sw846/online/index.htm>
520 [accessed 10 Mar 2012].

521 USDA Foreign Agriculture Service, 2010. GAIN report: National food safety standard -
522 maximum levels of contaminants in food [online]. URL
523 http://gain.fas.usda.gov/Recent%20GAIN%20Publications/National%20Food%20Safety%20Standard-Maximum%20Levels%20of%20Contaminants%20in%20Food_Beijing_China%20-%20Peoples%20Republic%20of_8-19-2010.pdf [accessed 24 Jan 2013].

527 Weisener, C.G., Smart, R., Gerson, A.R., 2003. Kinetics and mechanisms of the leaching of
528 low Fe sphalerite. *Geochim. Cosmochim. Acta* 67, 823–830.

529 Zhao, H., Xia, B., Fan, C., Zhao, P., Shen, S., 2012. Human health risk from soil heavy metal
530 contamination under different land uses near Dabaoshan mine, southern China. *Sci. Total. Environ.* 417-418, 45–54.

531 Zhao, L., Wu, L., Li, Y., Animesh, S., Zhu, D., Uphoff, N., 2010. Comparisons of yield, water
532 use efficiency, and soil microbial biomass as affected by the system of rice
533 intensification. *Commun. Soil Sci. Plant Anal.* 41, 1–12.

535 Zhuang, P., McBride, M., Xia, H., Li, N., Li, Z., 2009. Health risk from heavy metals via
536 consumption of food crops in the vicinity of Dabaoshan mine, south China. *Sci. Total. Environ.* 407, 1551–1561.

538 Zota, A.R., Willis, R., Jim, R., Norris, G.A., Shine, J.P., Duvall, R.M., Schaidler, L.A., Spengler,
539 J.D., 2009. Impact of mine waste on airborne respirable particulates in northeastern
540 Oklahoma, United States. *J. Air Waste Manag. Assoc.* 59, 1347–1357.

541

542 Table 1: **Characterisation data for the temperate and sub-tropical experimental**
 543 **soils.** Uncertainties reported as ± 1 standard deviation ($n = 5$). eCEC = Effective cation
 544 exchange capacity; LOI = Organic matter content, determined by loss on ignition.

	Temperate soil	Sub-tropical soil
pH	6.58 ± 0.07	6.83 ± 0.12
eCEC (cmol+ kg ⁻¹)	14.6 ± 0.3	13.1 ± 0.2
C _{organic} (% m/m)	5.57 ± 0.20	4.62 ± 0.06
C _{inorganic} (% m/m)	< LOD	0.47 ± 0.37
LOI (% m/m)	12.3 ± 0.5	13.1 ± 0.7
Al (mol kg ⁻¹)	1.44 ± 0.11	2.32 ± 0.11
Al _{oxalate} (mol kg ⁻¹)	0.121 ± 0.001	0.0975 ± 0.0018
Fe (mol kg ⁻¹)	0.973 ± 0.018	1.13 ± 0.03
Fe _{oxalate} (mol kg ⁻¹)	0.202 ± 0.002	0.0602 ± 0.0014
Mn (mmol kg ⁻¹)	37.6 ± 3.2	5.25 ± 0.31
S (mmol kg ⁻¹)	17.0 ± 2.2	17.1 ± 1.7
Cd (μ mol kg ⁻¹)	2.70 ± 0.55	2.67 ± 0.27
Zn (mmol kg ⁻¹)	2.05 ± 0.14	2.13 ± 0.17

545

546

547 Table 2: **Net Cd release (Cd_{net}) and percentage sphalerite dissolution** determined
 548 after 7 – 365 days incubation in both temperate and sub-tropical soils. Uncertainties are
 549 reported as ± 1 standard deviation ($n = 3$). Asterisks indicate insignificant differences
 550 between the spiked and control incubation values.

Days	Temperate soil		Sub-tropical soil	
	Cd_{net} (nmol Cd g⁻¹ ZnS)	% dissolution	Cd_{net} (nmol Cd g⁻¹ ZnS)	% dissolution
7	18.2 \pm 15.4	0.02 \pm 0.02	*	*
30	76.9 \pm 21.1	0.09 \pm 0.03	73.6 \pm 57	0.09 \pm 0.07
90	261 \pm 38	0.32 \pm 0.05	148 \pm 24	0.18 \pm 0.03
180	475 \pm 223	0.58 \pm 0.27	228 \pm 24	0.28 \pm 0.03
270	756 \pm 60	0.93 \pm 0.07	425 \pm 18	0.52 \pm 0.02
365	998 \pm 212	1.23 \pm 0.26	464 \pm 27	0.57 \pm 0.03

551

552 Figure 1: **Influence of microbiota upon soil pH:** Sulfate, pH (a) and nitrate (b) in biotic
553 and abiotic control incubations of the temperate soil. Uncertainties are reported as ± 1
554 standard deviation ($n = 3$).

555 Figure 2: **Redox indicators and metal availability in flooded paddy soils:** (a) SO_4^{2-}
556 and NO_3^- , (b) pH and Eh and (c) CaCl_2 -extractable Zn/Cd in the sub-tropical soil (180-
557 365 days), under both oxic (filled symbols) and anoxic (hollow symbols) conditions.
558 Uncertainties are reported as ± 1 standard deviation ($n = 3$).

559 Figure 3: **Cd and Zn release during sphalerite weathering:** CaCl_2 -extractable and
560 EDTA-extractable Cd (a/b_{I-II}) and Zn (a/b_{III-IV}) concentrations in temperate (a_{I-IV}) and
561 sub-tropical (b_{I-IV}) experimental soils. Uncertainties are reported as ± 1 standard
562 deviation ($n = 3$). Note that all Cd concentrations were below the detection limit (0.002
563 $\mu\text{mol Cd kg}^{-1}$) until day 180 of sub-tropical soil incubation (b_I). Asterisks denote
564 statistically significant ($p > 0.05$, ANOVA) differences between spiked and control soils.

565 Figure 4: **Plant uptake of cadmium:** total Cd tissue concentrations, stem
566 bioconcentration factors (BCF) based upon Cd_{net} concentrations and stem-to-grain
567 transfer factors (TF) for spring wheat grown in the temperate experimental soil and rice
568 in the flooded sub-tropical experimental soil. Uncertainties based on ± 1 standard
569 deviation.

570

571 Table S1: Certified and determined concentrations obtained for certified reference
 572 materials. Uncertainties are reported as ± 1 standard deviation ($n = 5$).

Χερτιφιεδ ματεριαλ	Παραμετερο	Χερτιφιεδ	Δετερμινεδ
IRMM 804 Rice flour	Cd ($\mu\text{mol kg}^{-1}$)	14.3 ± 0.6	14.3 ± 1.1
	Zn ($\mu\text{mol kg}^{-1}$)	353 ± 29	360 ± 32
BCR 320R Channel Sediment	Cd ($\mu\text{mol kg}^{-1}$)	23.5 ± 1.6	21.1 ± 0.2
	Zn (mmol kg^{-1})	4.88 ± 0.31	4.85 ± 0.19

573

574

575

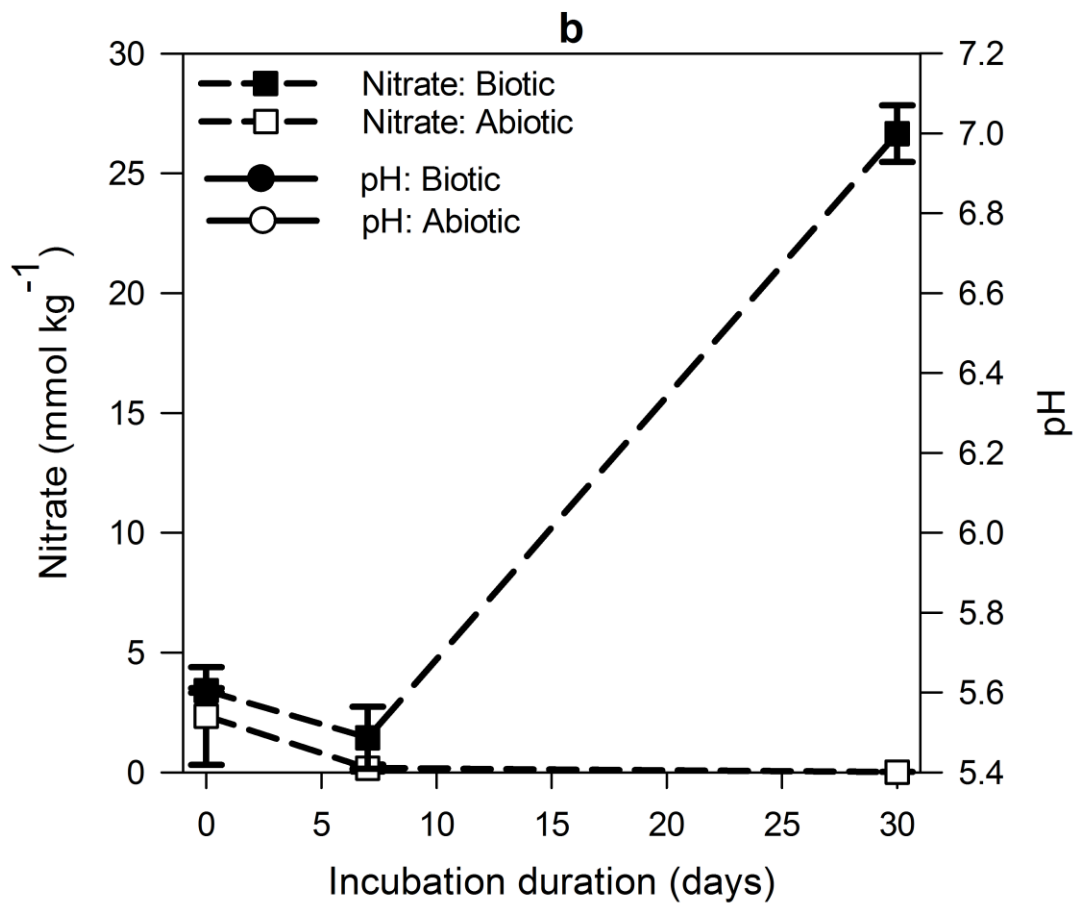
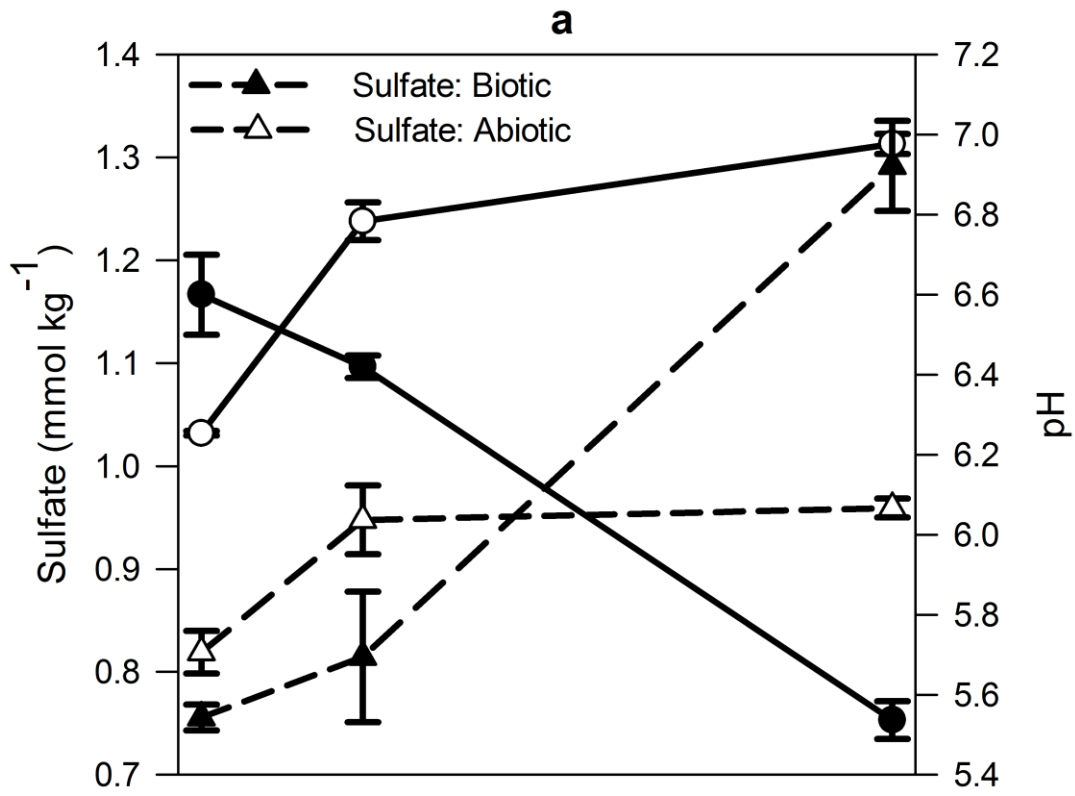
576 **Figure S1: XRD characterisation:** X-ray diffractogram obtained for the experimental
 577 sphalerite used in this study, plotted together with an exemplar pattern for wurtzite.

578

579

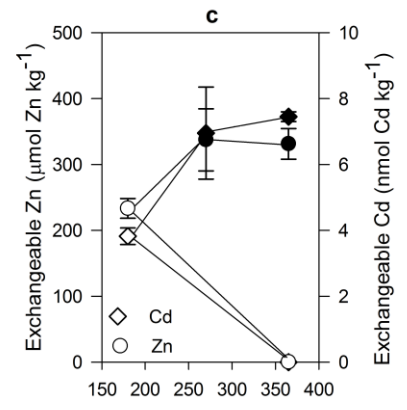
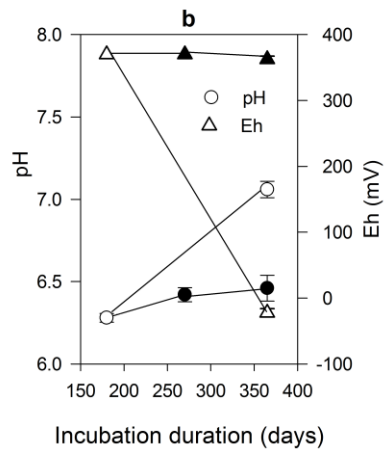
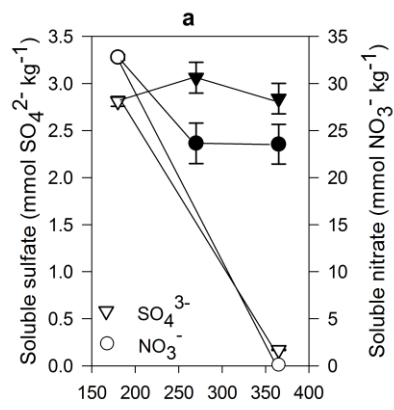
580 **Figure S2: Soil pH buffering curves for temperate and sub-tropical experimental**
 581 **soils:** The curves were produced by adding variable concentrations of H_2SO_4 (x-axis) to
 582 the soils and determining slurry pH after overnight equilibration (y-axis).

583



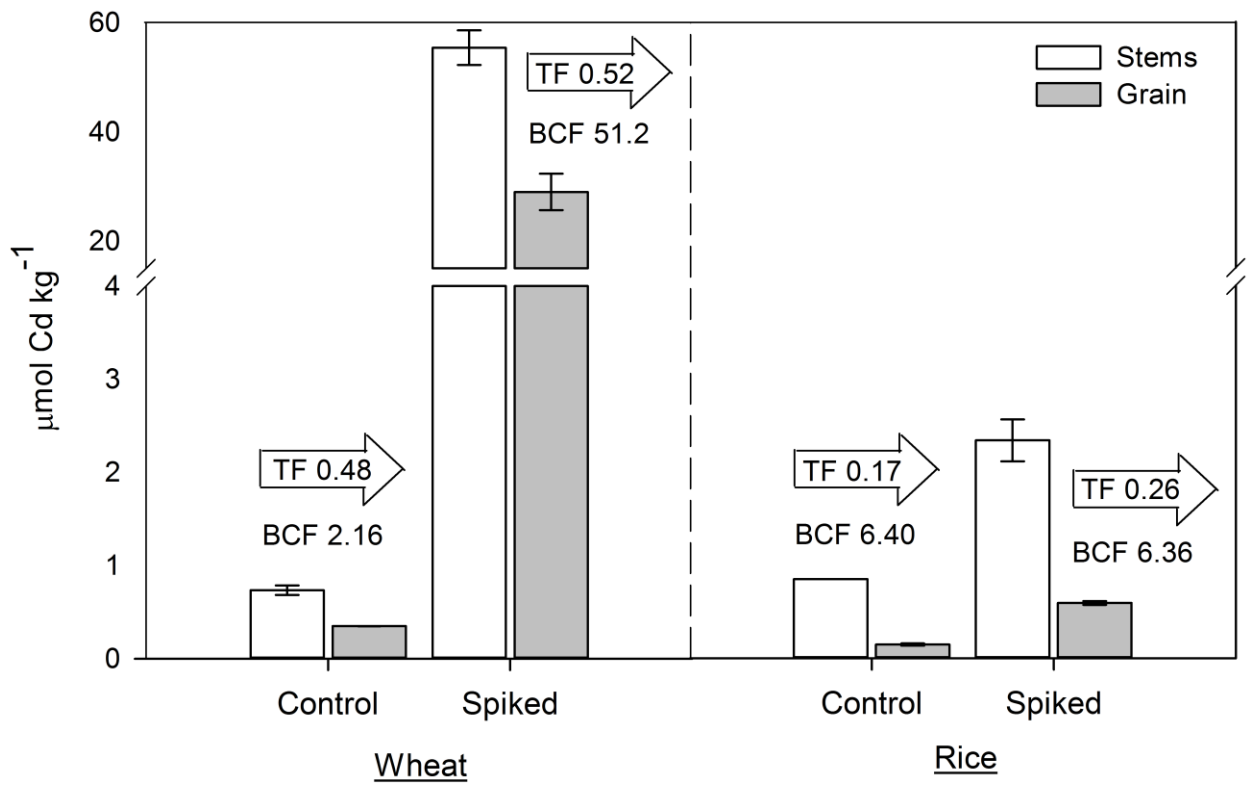
584

585



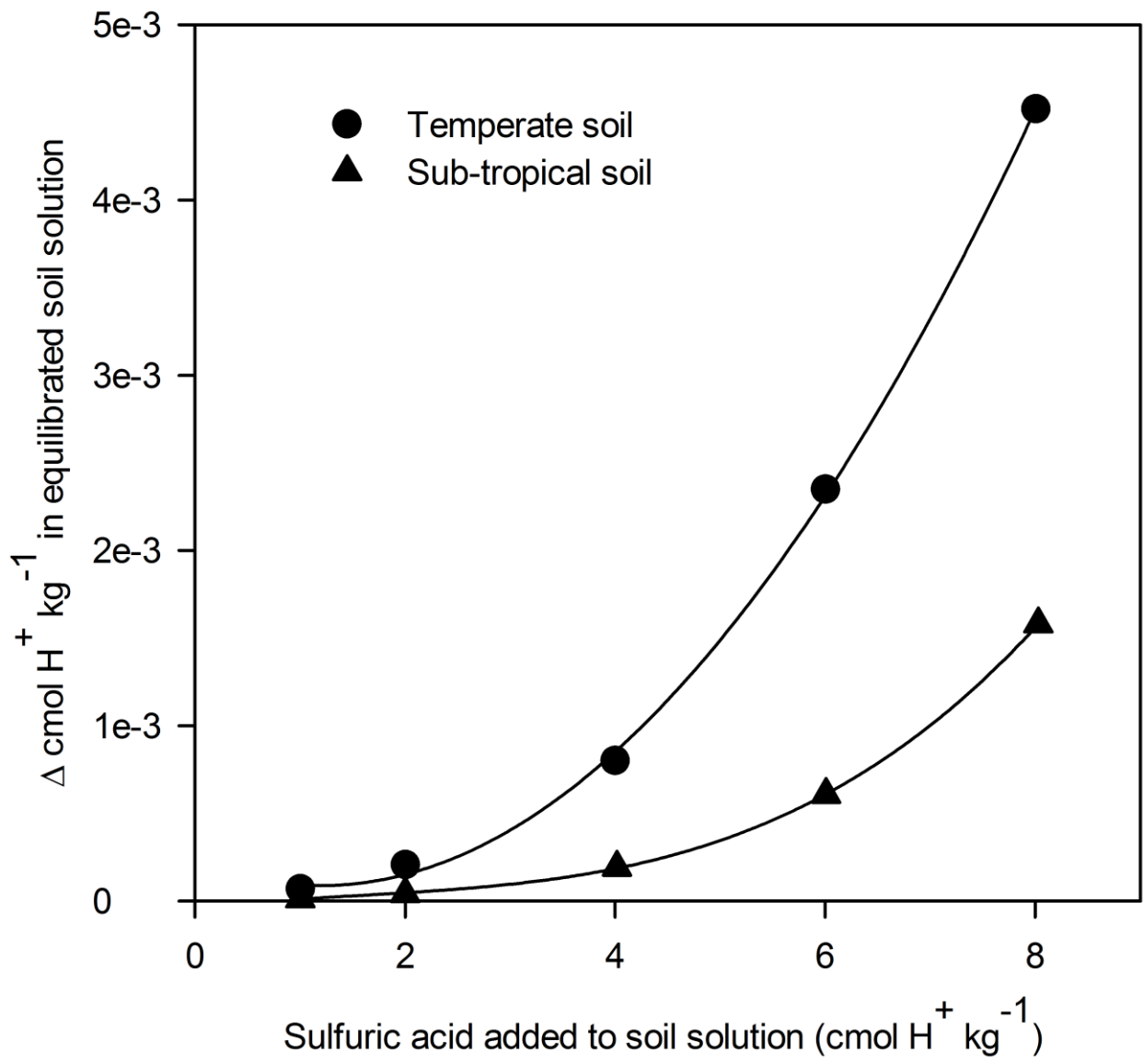
586

587



588

589



590